

Research article

Drought Index Assessment Using Thermal Vegetation Index (TVI) Method and Soil Physic Approaches (A Case study: Manyaran District, Central Java, Indonesia)

Mujiyo Mujiyo*, Dita Putri Mitayani, Dwi Priyo Ariyanto and Sumani

Department of Soil Science, Faculty of Agriculture, Universitas Sebelas Maret, Surakarta, Indonesia

Received: 18 October 2023, Revised: 24 October 2024, Accepted: 18 November 2024, Published: 9 December 2024

Abstract

The early detection of areas that have the potential to experience drought is necessary to minimize the hazards of land drought. The study aimed to identify the current conditions of drought by TVI with actual soil physic characteristic approaches, and to find the determinant factors related to the dynamics of agricultural land drought conditions so as to determine land management strategies that are considered appropriate and efficient to prevent agricultural land drought. The method for analyzing the drought index was the Thermal Vegetation Index (TVI) method, which involved the calculation of the ratio between the Land Surface Temperature (LST) and the vegetation index using Normalized Difference Vegetation Index (NDVI). The method in this research was modified by adding soil physical indicators, including soil moisture content, bulk density, and pF value. The results showed that the land drought classes were normal drought (46.89% study area), mild drought (20.62% study area), moderate drought (14.10% study area), severe drought (8.58% study area), and extreme drought (9.81% study area). Land drought was highly correlated to the soil's physical condition, negatively correlated with the moisture content ($r = -0.403$) and bulk density ($r = -0.317$), and positively correlated with the pF ($r = 0.429$). Enhancing the soil's capacity to absorb water and retain moisture through the addition of organic matter is one of the required techniques as a suitable recommendation to the issue after determining the determinant factors and present conditions.

Keywords: land surface temperature; Landsat 8; remote sensing; RETC; soil pF; vegetation index

1. Introduction

Drought is one of the natural disasters that, if not addressed, is very detrimental to various aspects of life—from the socio-economic sector to the agricultural industry. Drought causes health and financial problems, leading to a lower quality of life. Drought disrupts agricultural production, causing decreased crop yields, low water reserves in the soil, and the loss of water sources (Azadi et al., 2018). Farmers' yields tend to be lower during droughts, resulting in lower incomes and higher costs for cultivation inputs. In several cases in

*Corresponding author: E-mail: mujiyo@staff.uns.ac.id
<https://doi.org/10.55003/cast.2024.259463>

Copyright © 2024 by King Mongkut's Institute of Technology Ladkrabang, Thailand. This is an open access article under the CC BY-NC-ND license (<http://creativecommons.org/licenses/by-nc-nd/4.0/>).

countries in Asia, America, and Europe, drought occurs causing agricultural land to non-function optimally and to be converted into non-agricultural land.

Although droughts have usually had great negative impact, drought can provide clues for effective water management and conservation efforts (Lund et al., 2018) because drought is a recurring event. The handling of drought disasters in Indonesia is not yet equipped with information and identification data so the process is still very slow (Rahmawati et al., 2019). Early detection of drought is necessary, and the potential for drought can be analyzed using satellite imagery that identifies the temperature and vegetation of a land area. Conventional drought analysis has limitations in data coverage, so the best alternative is to use a geographic information system because it has greater effectiveness and wider data coverage. High-resolution satellite data has been proven to be a valuable data source for analyzing drought (Pandey et al., 2021).

Globally, the uneven distribution of rainfall is one of the causes of drought according to Libanda et al. (2019) who observed that during El Nino, rainfall decreases. During El Nino, rainfall intensity ranges from 0 to 20 mm, while under normal conditions, the rainfall intensity is 20 to 30 mm per day (Ryadi et al., 2019). Wonogiri Regency has been one of the areas affected by La Nina events since 2020 and is predicted to be affected by El Nino in 2023. Based on data from the Central Bureau Statistics of Wonogiri Regency (2022), agricultural land in Manyaran Sub-district, Wonogiri, occupies about 6,192.63 ha (76% of the total area of Wonogiri Regency), so a drought that occurs will result in huge losses for this region. Land use is dominated by agricultural landfills with high vegetation diversity and densities in this area; the denser the vegetation, the lower the drought index value.

There have been many previous studies on drought in Wonogiri. The methods used in previous studies varied but included were the Moisture Adequacy Index (MAI) method by Rahmawati et al. (2019) and the Standardized Precipitation Index (SPI) method by Ardiputro et al. (2016). The Thermal Vegetation Index (TVI) method has never been used before and there is no information yet on the level of drought in the research area. Drought prediction using the TVI method provides faster and more effective results because this method is obtained from satellite image processing, allowing for wide area coverage on a sub-district, provincial, and national scale. This research was conducted in more detail at the sub-district level, in addition to the soil physical properties approach. Soil physical properties are related to the ability of soil to retain water, which can affect water availability in the soil. Modifying soil physical properties can be done to increase the availability of soil water to overcome drought in the study area. Research analyzing land drought using the Thermal Vegetation Index (TVI) method in Manyaran Sub-district is important because the identification of drought can be done early and handled immediately. The purpose of this study was to analyze the drought index in the Manyaran area using the Thermal Vegetation Index (TVI) method, map the distribution of agricultural land drought, and examine the factors that determined the drought index in the Manyaran Sub-district. The research led to the formulation of recommendations for drought disaster mitigation to minimize the impact of drought.

2. Materials and Methods

This research used a descriptive method with Landsat 8 image interpretation based on remote sensing. The method used in determining the drought index involved the Thermal Vegetation Index (TVI). The research stages consisted of (1) Pre-survey; (2) Survey; and (3) Post-survey. In the pre-survey stages, a working map was made using land map units

(LMUs) obtained by overlaying thematic maps such as land use maps, soil type maps, rainfall maps, and slope maps. In the survey stage, the conditions in the study site were observed, Landsat 8 Image recording was performed, and soil samples were taken to identify the actual state of the soil (soil moisture, bulk density, and pH) in the laboratory. The final stage was the post-survey stage, which included sample preparation, laboratory analysis of soil samples, and correction of Landsat images starting with geometric correction, radiometric correction, and then classifying LST and scoring land drought classes.

Field observations to validate the image analysis results were studied by taking soil samples based on the LMU (Figure 1). Sampling was carried out by purposive sampling at 21 LMUs, with 3 sampling points per LMU, and the observation points totaled 63 points. The modification made in this study was to create more profound observations on soil parameters, including soil texture, bulk density, and soil moisture content. Laboratory analysis was conducted on soil texture, bulk density (Bd), and moisture content. The three parameters were used to calculate the soil pH values using the Van Genuchten Mualem calculation method. The method used for soil texture analysis was the pipette method, while the actual soil moisture content was analyzed by the gravimetric method.

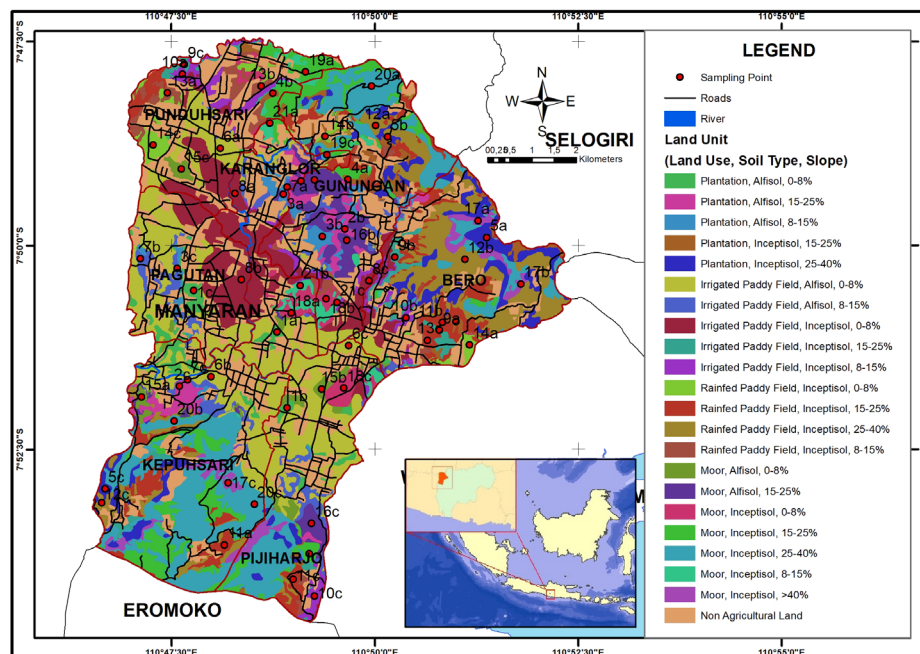


Figure 1. Land Map Unit (LMU)

2.1 Data analysis for land drought classification

2.1.1 Radiometric correction

Radiometric correction is performed to correct pixel values due to radiometric errors. These errors can be caused by the sun's location or recording angle differences. The correction was done by converting DN values into reflectance spectral unit values.

2.1.2 Land surface temperature (LST) classification

Land Surface Temperature was calculated with the brightness temperature method using band ten or the thermal band on the Landsat 8 image. The purpose of this calculation was to determine the land surface temperature. The results of the LST calculation in Celsius were used to calculate the TVI values with equation (6).

2.1.2.1 Conversion of the digital number to radiance

The first stage was to convert each digital number value in the image into a radian value. The goal was to correct the pixel value in the image due to the influence of atmospheric disturbance factors. The results of the radian values were then used to calculate the LST values. The radiance values were calculated using equation (1) (USGS, 2015).

$$L\lambda = ML * Q_{cal} + AL \quad (1)$$

Description:

$L\lambda$ = Spectral radiance (Watts/(m²* srad * μ m))
 ML = Band-specific multiplicative rescaling factor from the metadata
 AL = Band-specific additive rescaling factor from the metadata
 Q_{cal} = Pixel value of the calibrated standard product (DN)

2.1.2.2 Conversion of radiance value to LST

Each radian value was then converted into an LST value using equation (2) (USGS, 2015), which was in Kelvin units and had to be converted to Celsius units.

$$T(K) = \frac{K2}{\ln\left(\frac{K1}{L\lambda}\right) + 1} \quad (2)$$

Description:

$T(K)$ = Land surface temperature (Kelvin)
 $K1$ = Calibration constants from metadata
 $K2$ = Calibration constants from metadata
 $L\lambda$ = Spectral radiance

2.1.2.3 Conversion of surface temperature from Kelvin to Celsius units

The unit of temperature value used was Celsius so the temperature had to be converted from Kelvin to Celsius with equation (3).

$$T(^{\circ}C) = T(K) - 273 \quad (3)$$

Description:

$T(^{\circ}C)$ = Land surface temperature ($^{\circ}C$)
 $T(K)$ = Land surface temperature (Kelvin)

2.1.2.4 Classification of LST value

The LST values were classified into five classes, and the interval of each class was obtained by equation (4).

$$Interval = \frac{(Max\ LST\ value - Min\ LST\ value)}{Number\ of\ class} \quad (4)$$

2.1.3 NDVI value classification

The Normalized Difference Vegetation Index (NDVI) combines image enhancement and subtraction techniques. The NDVI method provides high quality results for vegetation with variable density and scattered vegetation from multispectral remote sensing images (Jones & Vaughan, 2010). The formula for calculating NDVI values is shown in equation (5) (Orhan et al., 2014).

$$NDVI = \frac{(NIR - RED)}{(NIR + RED)} \quad (5)$$

Description:

NDVI = Value from Normalized Difference Vegetation Index
 NIR = Reflectance value of the near-infrared band
 RED = Reflectance value of the red band

2.1.4 Determination of drought index

The calculation of drought index was carried out using the Thermal Vegetation Index method obtained from the ratio of LST value and NDVI value with equation (6) (Bhandari et al., 2012), which was then classified according to TVI in Table 1.

$$TVI = \frac{LST}{NDVI} \quad (6)$$

Description:

TVI = Value of the thermal Vegetation Index
 LST = Land Surface Temperature Value
 NDVI = Normalized Difference Vegetation Index Value

Table 1. Classification of TVI research areas

No.	Drought Class	TVI Value
1.	Normal	0 – 55
2.	Mild	55 – 70
3.	Moderate	70 – 85
4.	Severe	85 – 99
5.	Extreme	>99

Source: Domiri (2006) & Munir et al. (2015)

2.1.5 Validation

Validation was done by comparing the drought values from the image analysis with the drought values in the actual condition based on the calculation of soil pF of the study area. The soil pF value was calculated using Van Genuchten Mualem calculation (van Genuchten, 1980) as described in equations (7) and (8).

$$|h| = \frac{n \left(\frac{1 - 1/n}{\sqrt{\theta_s - \theta_r}} \right)^{-1}}{|\alpha|} \quad (7)$$

$$pF = \log_{10} h \quad (8)$$

Description:

- h = hydraulic conductivity
- θ_{act} = actual moisture content (cm³/cm³)
- θ_s = saturated moisture content (cm³/cm³)
- θ_r = residual moisture content (cm³/cm³)
- n, α = fitting parameters

The values of θ_s , θ_r , n , and α , were obtained from the RETC application by input of the values of soil texture and bulk density (BD). RETC is a program that provides data on soil hydraulic conductivity parameters and accurately describes soil water retention (Yates et al., 1992). The calculated pF values were then classified according to the parameter values of the soil water retention curve (shown in Table 2) (Taufik & Setiawan, 2012).

Table 2. Drought index value based on pF value

Soil Water Retention Curve Parameters	pF	Drought Index
Saturated	0.2	Normal
Air-entry	1.8	Mild
Field capacity	2.5	Moderate
Critical point	3.1	Severe
Permanent wilting point	4.2	Extreme drought

A confusion matrix was used to calculate the accuracy values, which calculated the number of points that produce the similar value of drought index between image analysis and field results based on pF values. An accuracy value greater than 70% was considered acceptable (Congalton, 1991).

2.2 Statistical analysis

Data were analyzed using ANOVA to determine the effect of land characteristics on the drought index, and if the values were significant, the test was then continued using DMRT test. Determinant factors of drought index were conducted using Pearson's correlation test, which describes the relationship between soil physical characteristics and the drought index.

3. Results and Discussion

3.1 Radiometric correction

The digital number (DN) values before radiometric correction for the multispectral band ranged from 0 to 65,535, while after radiometric correction, the DN values ranged from 0 to 1.329378. Figure 2 shows the visual difference between the images before and after radiometric correction. The corrected image had a higher contrast so it was easier to analyze. Visually, the image quality is higher because the pixel values in the image are closer to the normal pixel values.

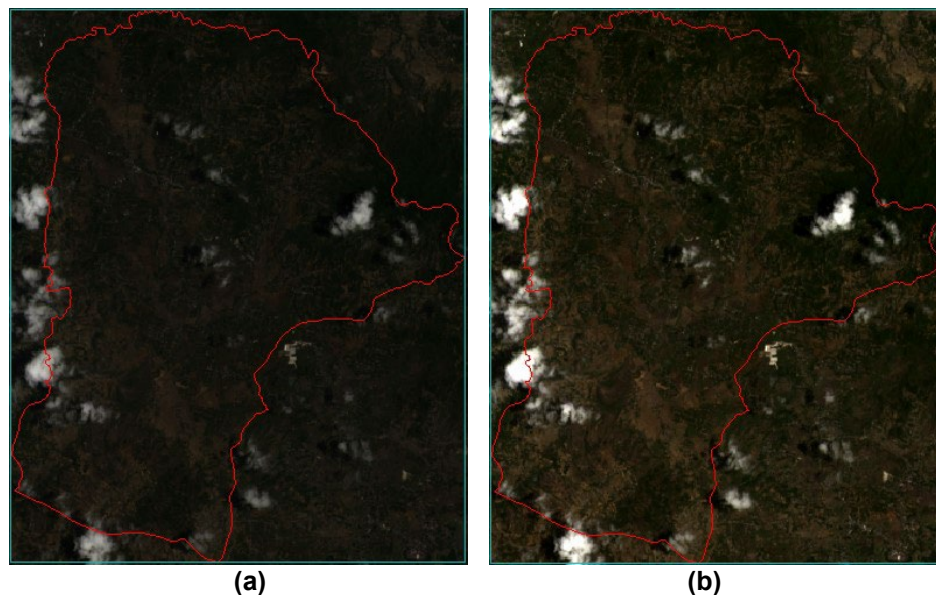


Figure 2. (a) Before radiometric correction (b) After radiometric correction

3.2 The distribution of land surface temperature (LST)

The LST processing results showed that the lowest DN value in the study area was 16.4°C and the highest was 34.2°C, so the average LST was 26.9°C. Satellite images were taken at 09:42 Western Indonesian Time (or WIB) when the sun was not high, and the LST was still relatively in the low temperature range. The research results of Rajeshwari & Mani (2014) showed that areas with high vegetation density had low LST values, while open land with no tillage soil or urban areas had high LST values. The LST value is produced from the sun's heat falling on the earth and being absorbed by the surface of the soil temperature. Therefore, non-agricultural lands in the form of open land, settlements, industrial sites and areas with dense distribution of buildings without vegetation, as well as highway areas, have a higher LST rate compared to land used for forests, paddy fields, plantations, and water bodies that have a LST rate that tends to be lower (Xiao et al., 2008).

The dominant LST value in the study area was 24 to 27°C, with an area of 2,832 ha or 45.62%. In a small part of the study area (56 ha), the LST was only in the range of 16-19°C, and other land areas (517 ha) had LST in the 20 to 23°C range (Figure 3). The

highest temperature was 28 to 33°C, distributed over 2,802 ha or about 45.14% of the study area. According to Central Bureau Statistics of Wonogiri Regency (2022), the average air temperature in November 2022 (the research process was conducted using satellite imagery) was 27.5°C. This value was close to the average LST value and it also can be concluded that this study demonstrated that air temperature influenced soil. Soil temperature increases as air temperature and light intensity increase (Alqudsi, 2021).

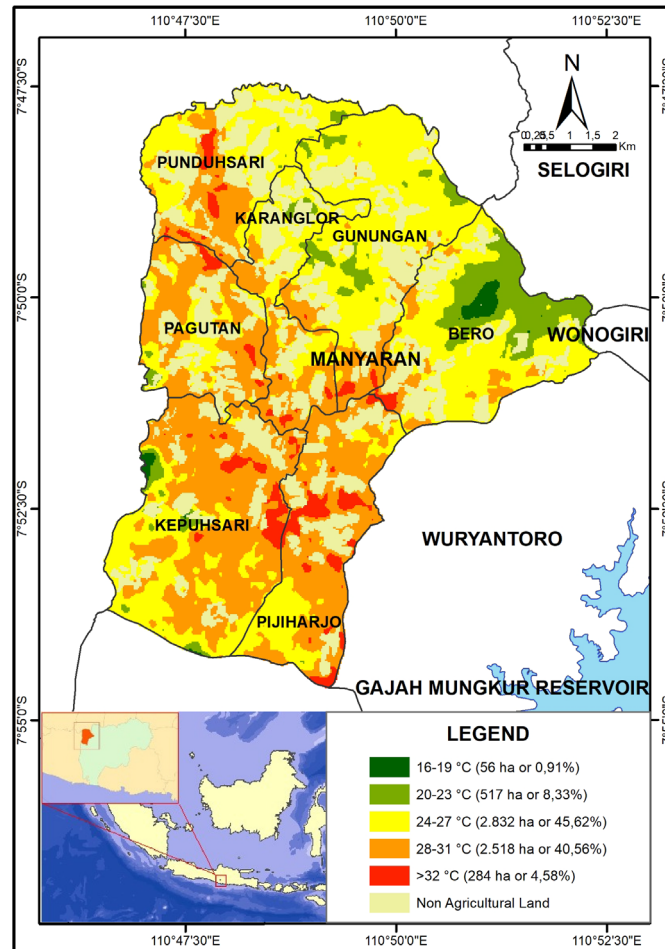


Figure 3. Distribution of land surface temperature

3.3 The distribution of NDVI

NDVI was used to monitor the vegetation level of the land, as seen from the greenish color produced on the image. The results show the lowest value of the vegetation index (NDVI) in the Manyaran Sub-district was 0.062, and the highest value was 0.793, so overall the average index of NDVI was 0.493. The range of vegetation index shows that most of the study area had a high level of greenness. The higher the NDVI value, the higher the chlorophyll and biomass of a vegetation object (Khanh et al., 2020). The lowest value of

NDVI was found in areas with little vegetation (Gandhi et al., 2015). The type, stand density, and vegetation age can influence NDVI values, because age stands will face recession, slow growth, and even wither to death, so vegetation at a productive age has a higher NDVI score (Lin et al., 2008). The average NDVI value for plantations was the highest when compared to other land uses. The plantation was dominated by perennial plants that have dense leaves, so the NDVI value was high.

The NDVI processing results showed that an area of 4,991 ha or 80% of the study had a high level of greenness (Figure 4). Plantations dominated the high greenness level, suggesting that there was a significant density of vegetation at site location. A high NDVI number indicates that the site is used for agriculture or forests (Mohajane et al., 2017). Only a small part of the land, in 26 hectares or 0.42% of the total study area, had a poor level of greenness, indicating extremely limited vegetation. In contrast, 1,016 ha or 16.37%, and 174 ha or 2.81% of the entire effective research area, respectively, had moderate and low levels of greenness. Low NDVI values can result from water stress in plants at different phases of plant phenology (Silva et al., 2016).

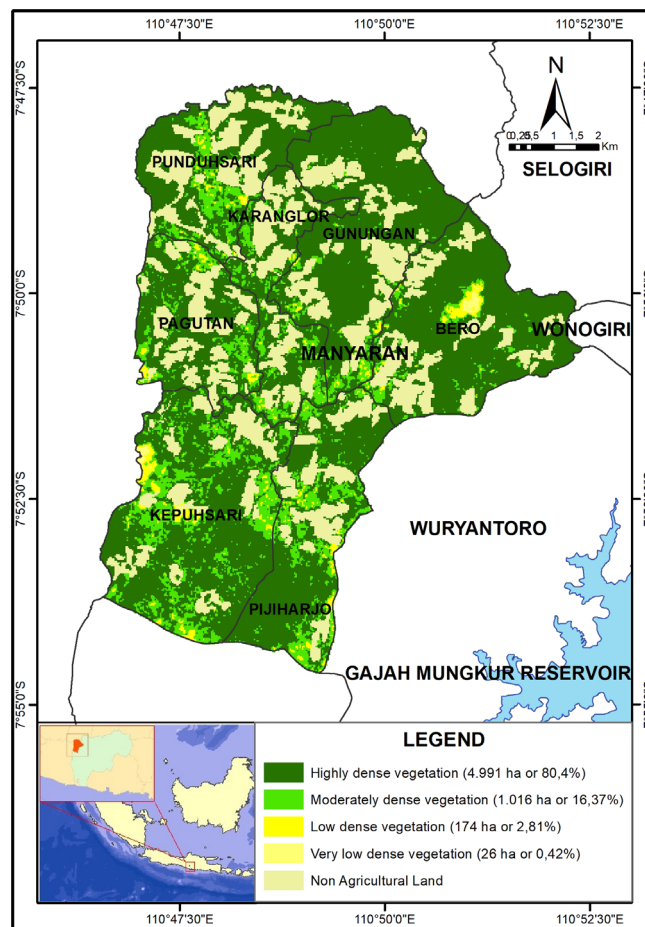


Figure 4. Distribution of NDVI

3.4 The distribution of drought

Figure 5 shows that the area classified as having a normal drought index was the largest of the classes, taking up 2,911 ha, or 46.89% of the total study area. Areas with mild and moderate drought indices were also quite large, amounting to 1,280 ha or 20.62% and 875 ha or 14.10%, respectively. Meanwhile, areas with severe and extreme drought indices only amounted to 532 ha or 8.58% and 609 ha or 9.81%, respectively, of the total study area.

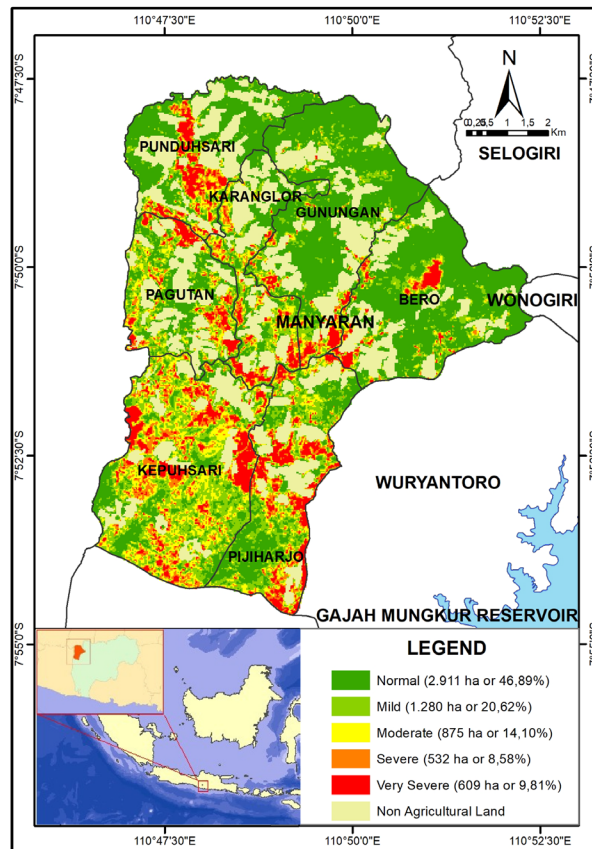


Figure 5. Distribution of land drought in study area

A normal drought index dominated the plantation area of 80.56%. Trees of perennial plants with a canopy made up the majority of the vegetation in the plantation area. According to Yeneneh et al., (2022) land covered by canopy has a low LST value and a high NDVI value, which results in a low drought index (Sruthi & Aslam, 2015). Meanwhile, a mild drought index was present in 11.8% of the plantation area. Only a small percentage of the farm had moderate, severe, or extreme drought index (4.23%, 1.83%, and 1.57%, respectively). Different species that create a litter with distinct qualities make up plantation vegetation. The decomposition of several types of litter is a source of soil organic matter, so it can play a role in water conservation (Ding et al., 2023).

The moor had a normal drought index with a percentage of 50.25% of the moorland. Moorland is dominated by vegetation found in dryland farming systems, agricultural systems with limited water use, and area that only rely on rainwater (Nurdin, 2011). The secondary crops that were grown in the dryland of the study area had the advantage of needing minimal water, allowing them to thrive during dry seasons and with little precipitation. According the research results of Dariah & Heryani (2014), depending on rainfall, secondary crops only need 2 to 3 mm of irrigation each day. The moor area's mild drought index was 24.38% of the total moor area. The NDVI value was not very high because the moor areas typically have a moderate vegetation density (Hidayati, 2013). Compared to aquatic bodies, crops, and forests, moors have a higher LST value (Deng et al., 2018). In the moor area, the percentages for moderate, severe, and extreme drought index were 14.89%, 6.31%, and 4.16%, respectively. The NDVI were low since some of the moor areas were yet unplanted or the plants were still immature.

According to the results of the DMRT, the average drought index for irrigated paddy fields was 45.57a, which was considerably different from the average drought index for other land uses (shown in Figure 6). However, 22.54% of the study area was made up primarily of site with normal drought index. Additionally, 21.97%, 19.37%, 14.71%, and 21.38% of paddy fields were mild, moderate, severe, and extreme drought zones, respectively. The land was in various stages of management since paddy planting was not done all at once. The findings revealed that variations in the planting season caused visual variances in the images (Tatisina et al., 2020). The link between LST and NDVI is mostly influenced by radiation during the start and finish of the growing season, with biophysical parameters having a negligible impact (Karnieli et al., 2010). With 61.91% of the total area of rainfed paddy fields, the majority of these fields had a normal drought index. Additionally, mild drought was present throughout 16.93% of the paddy fields area. Rainfed paddy fields' drought indexes were divided into three categories: moderate (10.12%), severe (6.07%), and extreme (4.94%).

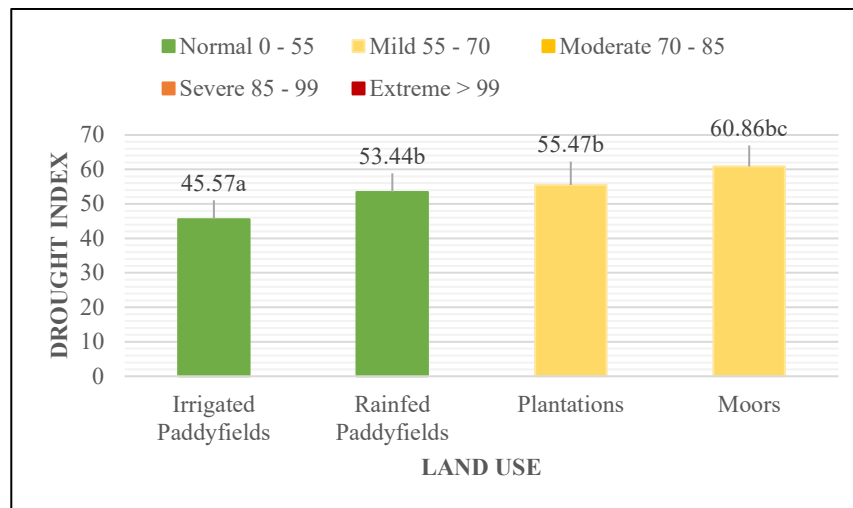


Figure 6. Land drought index under different types of land use

Remarks: Numbers followed by different letters are interpreted as having a significant difference.

Using a confusion matrix, the accuracy of the TVI approach in assessing drought was determined by adding up the sites that yielded identical drought index based on field and image analysis results (Table 3). The field is experiencing drought, according to the pF value. The 63 sampling sites had different pF values. A state between saturated and water-entry sites was indicated for 34 sites with pF values between 0.2 and 1.8, indicating normal drought levels. A condition between water-entry and field capacity was indicated for 25 sites with pF values between 1.8 and 2.5, indicating that they were at a mild drought level. A condition between field capacity and the critical point, or moderate drought, was indicated for four more locations with pF values between 2.5 and 3.1.

Table 3. Confusion matrix

Class		Imagery Analysis Results					Total
		Normal	Mild	Moderate	Severe	Extreme Drought	
Research Results	Normal	31*	2	1	0	0	34
	Mild	2	23*	0	0	0	25
	Moderate	0	1	3*	0	0	4
	Severe	0	0	0	0*	0	0
	Extreme drought	0	0	0	0	0*	0
	Total	33	26	4	0	0	63

*The number of samples that resulted in the same drought classification between the image and laboratory analysis results. This value is then used to calculate the overall accuracy.

The overall accuracy value can be calculated as shown in equation (9) (Congalton, 1991):

$$OA = \frac{(31+23+3+0+0)}{63} \times 100\% \quad (9)$$

$$= 90.48 \%$$

Based on the calculation using the above equation, the image accuracy value obtained was 90.48%, meaning that the results of image analyses were acceptable.

3.5 Soil physical properties and their relationship with the land drought index

Changes in the climate and surroundings can alter the properties of soil, necessitating adaptation to preserve the capacity to sustain plant development (Utami et al., 2024). Determining variables for managing drought can be found in soil properties that have significant correlation with the drought index. The results showed that the soil texture of the study area was classified into eight texture classes: clay, silty clay, clay loam, silty clay loam, silty loam, loam, sandy loam, and sandy clay loam. The clay and clay loam soil types dominated the soil texture of the study area. Soil bulk density values varied from the lowest of 0.88 g/cm³ to the highest of 1.31 g/cm³, with an average density of 1.10 g/cm³ (Table 4). The highest bulk density value soil had a clay texture, while the lowest had a sandy loam texture.

Table 4. Texture, bulk density, moisture content, and pF condition at each sampling point

Point	Texture (%)			Bulk density	Moisture content	pF	Point	Texture (%)			Bulk density	Moisture content	pF	Point	Texture (%)			Bulk density	Moisture content	pF
	Silt	Clay	Sand					Silt	Clay	Sand					Silt	Clay	Sand			
1A	34.95	58.38	6.67	1.15	0.52	1.48	8A	42.52	50.24	7.24	1.13	0.55	0.94	15A	29.11	27.42	43.46	1.17	0.38	2.04
1B	41.79	52.96	5.25	1.17	0.47	1.89	8B	18.73	75.03	6.24	1.19	0.50	1.70	15B	50.52	38.23	11.25	1.12	0.53	1.26
1C	47.39	43.12	9.50	0.99	0.50	1.88	8C	38.42	46.60	14.97	1.29	0.48	1.34	15C	25.84	66.70	7.47	1.00	0.44	2.28
2A	36.15	32.69	31.16	1.15	0.46	1.71	9A	34.02	57.44	8.54	1.19	0.53	1.23	16A	26.61	10.06	63.33	0.88	0.42	1.92
2B	36.40	27.46	36.15	0.97	0.37	2.34	9B	39.54	53.97	6.49	1.16	0.53	1.29	16B	28.60	27.97	43.43	1.11	0.48	1.39
2C	36.63	31.95	31.42	1.23	0.39	2.03	9C	40.35	47.70	11.94	1.20	0.49	1.58	16C	41.08	42.42	16.50	0.94	0.50	1.88
3A	33.85	45.69	20.46	1.06	0.50	1.73	10A	50.40	27.83	21.77	1.11	0.52	0.00	17A	35.87	25.68	38.45	0.98	0.49	1.73
3B	36.98	33.45	29.57	1.29	0.49	0.00	10B	50.57	38.75	10.69	1.19	0.44	2.15	17B	41.74	16.95	41.31	1.06	0.41	2.02
3C	28.16	69.28	2.56	0.92	0.42	2.55	10C	36.00	43.69	20.31	1.08	0.56	0.00	17C	27.78	18.11	54.11	1.27	0.47	0.00
4A	44.09	37.05	18.86	1.15	0.47	1.77	11A	27.53	45.93	26.54	1.14	0.49	1.53	18A	21.96	70.84	7.20	1.13	0.49	1.83
4B	48.21	40.82	10.96	1.21	0.48	1.66	11B	34.93	35.05	30.02	0.97	0.31	2.64	18B	18.98	68.08	12.94	1.16	0.39	2.44
4C	62.66	22.84	14.49	1.18	0.45	1.86	11C	28.78	37.44	33.78	1.15	0.51	0.89	18C	26.49	48.19	25.32	1.11	0.50	1.59
5A	41.52	23.19	35.29	1.07	0.44	1.88	12A	35.05	42.10	22.86	1.24	0.46	1.62	19A	39.65	36.69	23.66	1.05	0.41	2.16
5B	52.60	23.85	23.55	0.90	0.51	1.86	12B	28.85	21.11	50.04	1.12	0.52	0.00	19B	35.66	46.98	17.36	1.10	0.51	1.52
5C	62.87	17.92	19.21	1.18	0.34	2.43	12C	34.10	36.04	29.87	1.06	0.51	1.52	19C	49.92	11.14	38.95	1.25	0.38	1.78
6A	59.92	13.18	26.90	1.10	0.53	0.00	13A	50.04	43.12	6.84	1.16	0.44	2.02	20A	33.21	39.47	27.32	1.01	0.42	2.16
6B	41.48	35.83	22.69	1.00	0.54	1.43	13B	30.11	47.92	21.97	1.32	0.39	2.06	20B	31.37	30.49	38.14	0.90	0.49	1.85
6C	47.82	43.15	9.03	1.15	0.49	1.68	13C	35.02	47.93	17.05	1.13	0.37	2.37	20C	14.42	21.64	63.94	1.27	0.36	1.83
7A	47.44	47.78	4.78	1.16	0.51	1.53	14A	38.96	53.95	7.08	1.02	0.44	2.21	21A	22.88	32.00	45.12	1.12	0.46	1.64
7B	31.62	62.21	6.17	0.92	0.55	1.72	14B	47.25	30.41	22.34	1.03	0.55	0.00	21B	20.90	72.89	6.21	1.02	0.41	2.54
7C	26.03	61.96	12.01	0.95	0.59	1.31	14C	22.14	70.39	7.47	1.08	0.50	1.85	21C	5.91	88.90	5.20	1.14	0.41	2.54

Remark: Silt (0.002 – 0.05 mm); Clay (<0.002 mm); Sand (0.05 – 2 mm); Bulk density (gr/cm³); Moisture content (cm³/cm³)

The actual moisture content values ranged from 0.31 cm³/cm³ to 0.58 cm³/cm³, with an average value of 0.47 cm³/cm³. The lowest moisture content value was found for soil with a silty clay texture with a bulk density value of 0.97 g/cm³, while the highest was of a clay texture with a bulk density value of 0.95 g/cm³. The lowest pF value was 0.0, which was found in soil that was saturated with water, while the highest was 2.63, corresponding to soil at field capacity conditions.

The parameters of soil physical properties and drought index having a significant correlation were determinants of land drought index in the study area. The strength or weakness of the correlation between soil physical properties and drought index is indicated by the R-value or Pearson value (shown in Table 5), and the average value of each drought factor parameter for various land uses can be seen in Figure 7.

Table 5. Correlation between soil physical properties and drought index

Soil Parameters	R	P-value
Bulk Density	-0.317*	<0.05
Moisture Content	-0.403**	<0.01
pF	0.429**	<0.01

*) means significant correlation at 95% (p-value ≤ 0.05)

**) means significant correlation at 99% (p-value ≤ 0.01)

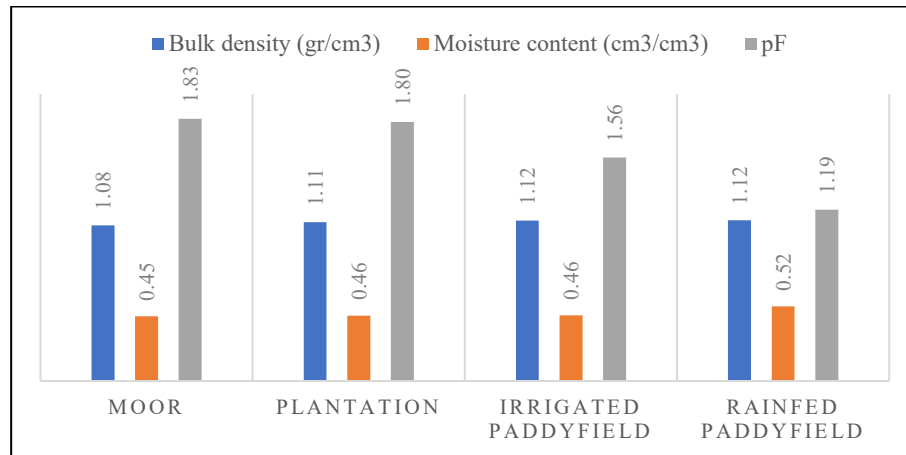


Figure 7. Average soil physics indicator values under different types of land use

According to the correlation analysis's findings, there were both positive and negative correlations with significant values. The drought index and soil bulk density had a substantial negative correlation; that is, the greater soil bulk density value, the lower drought index in the area. This means that the higher the soil bulk density value, the higher the soil adhesion force. A high bulk density value means that the soil has a small particle size (Bhavaya et al., 2018), which causes the pore size distribution to increase and has a significant water-holding capacity (El-Nagar & Mohamed, 2019). While, the soil adhesion

force was positively correlated with soil moisture (Zheng et al., 2021). The regression equation for the drought index was obtained and is shown in equation (10).

$$\text{Drought Index} = 115.16 - 30.620 \text{ Bulk Density} - 62.192 \text{ Soil moisture} + 1.485 \text{ pF} \quad (10)$$

The drought index and the moisture content parameter had a negative correlation meaning that the greater the drought index, the lower moisture content value. A thorough study of the soil's moisture content can detect drought (Ladányi et al., 2021). Moisture content was also influenced by land use (p-value < 0.05), and irrigated paddy fields had the lowest drought index value. At the time of soil sampling, irrigated paddy fields were in the inundation phase. Inundation can reduce soil percolation so that there is less water loss (Mohanty et al., 2004). Lack of water in the soil causes plant death and a decrease in the quality of the harvest (Neamah et al., 2023).

The drought index and the pF parameter showed a highly significant positive correlation, meaning that the more severe the drought, or the higher the pF value, the higher drought index. Soil water retention, or its capacity to retain water, is reduced during droughts compared to normal circumstances (Fujihara et al., 2013). The pF value was also influenced by land use (p-value < 0.05). The land use with the highest pF value was the moor, with a pF value of 1.83, while the lowest pF value was found for the irrigated paddy, with a pF value of 1.19. Water retention (pF curve) is influenced by soil particle size, the finer the soil particles, the greater the water-holding capacity (Robinson et al., 2016). Irrigated paddy fields were cultivated more intensively than moorland. Intensively cultivated land has less sand than land with a no-tillage system (Qi et al., 2018). The sand fraction is broken up due to the processing process and becomes a smaller fraction of dust or clay.

3.6 Drought mitigation recommendations

Drought due to changes in global temperatures and rainfall patterns is very detrimental to various environmental sectors such as degradation of landforms (Wahyuti et al., 2023), expansion of critical land and especially agricultural land (Sengupta & Thangavel, 2023), and reduction in the quality and nutrient content of agricultural products (Rusdin et al., 2023). Mitigation efforts can be made, especially on moorland, because it has the highest drought index value by considering the physical properties of the soil, especially moisture content and pF, which are the determining factors of drought. Efforts can be made to improve the soil capability to absorb water and maintain moisture by adding organic matter (Rahayu et al., 2024). Adding organic carbon reduces water and nutrient losses due to erosion (Chaudhari et al., 2015) and increases the soil's capacity to hold water (Hugar et al., 2012), to reduce the risk of solid soil and inundated land by rainwater (Romadhon & Aziz, 2022). Other efforts that can be made are the additions of mulch and cover crops. The application of mulch can reduce soil surface temperature (Minasny & McBratney, 2017), and increase soil moisture content. Land tillage with added organic fertilizer also has physicochemical soil properties that support soil moisture recovery (Kurniawan et al., 2023) and improve soil fertility (Hakimi & Hamdoun, 2023).

Meanwhile, residues produced from cover crops can reduce water loss due to evaporation (Mangani et al., 2022). Planting edge crops can also be used to reduce soil water loss. Peripheral plants can function as windbreakers so that the wind hitting the ground is not too strong, thus reducing high evapotranspiration and evaporation (Meyer et al., 2019; Veste et al., 2020). Drought conditions at the study area in normal and mild index level allow the cultivation of crops with high drought resistance such as sorghum (*Sorghum*

bicolor (L.) Moench), sweet corn (*Zea mays* L. *Saccharata* Sturt), and sugarcane (*Saccharum officinarum* L.). Chaniago et al. (2017) found that the sorghum genotypes Samurai 2 and Pahat Batan were tolerant to drought stress treatment with resistance probability values ranging from 48.8 to 54.30%, because the root lengths were still prominent even in drought stress treatment so that it can support plant growth by absorbing water and nutrients from the soil. Both sorghum genotypes have drought tolerance capabilities of 84 to 100% respectively.

Drought mitigation can also be done by utilizing existing water sources effectively and efficiently. Utilization of land irrigation should be done with consideration of the sustainability of groundwater sources and soil aquifers (Monfared et al., 2019). Information related to the location and discharge of water sources can benefit agricultural land water distribution. However, the coverage of geospatial data on water sources in developing countries is relatively limited (Anshori et al., 2023). Previously, it was necessary to survey unexplored locations to improve the water point database. In the future, it will be essential to conduct mapping related to water sources in Manyaran Sub-district. Mapping can provide an overview of the availability and accessibility of water sources (Yu et al., 2019; Anusha et al., 2022), and provide guidelines for the sustainably management of water sources (Li et al., 2023). Proper management of water sources can provide solutions so that water can be evenly distributed from upstream to downstream (Goonetilleke & Vithanage, 2017).

4. Conclusions

The distribution of the land drought index in the Manyaran Sub-district was divided into five classes: normal drought covering 2,911 ha (46.89%), mild drought covering 1,280 ha (20.62%), moderate drought covering 875 ha (14.10%), severe drought covering 532 ha (8.58%), and extreme drought covering 609 ha (9.09%). Land use had an effect on drought in the Manyaran Sub-district. The maximum drought value was associated with moorlands, while the lowest was with the irrigated paddy fields. The moisture content and pF value also determined the degree of desertification in the study area. When moisture content was greater, dehydration was reduced. In contrast, there was a direct relationship between drought and pF, the greater the pF value, the more severe the shortage. Adding organic matter to increase soil moisture content and decrease pF value, as well as using mulch, edge crops, and shade, are drought mitigation measures that can be implemented in the Manyaran area and in areas with similar land characteristics. Future implications of this research include monitoring drought trends and land vegetation density for the region from year to year and researching accurately and effectively the physical conditions of the soil that influence the quantity of water flow to the soil. By identifying current requirements and factors, researchers should concentrate more on developing the necessary strategies and targeted solutions to the problem of land drought. Future catastrophic droughts will be prevented or mitigated as expeditiously as possible by means developed and implemented.

5. Acknowledgements


The authors would like to thank the General Directorate of Higher Education, Research and Technology – Ministry of Education, Culture, Research and Technology for the research funding provided through the 2024 Regular Fundamental Research scheme with the number 1076.1/UN27.22/PT.01.03/2024.


6. Conflicts of Interest

There is no conflict.

ORCID

Mujiyo  <https://orcid.org/0000-0002-6161-7771>

Dita Putri Mitayani  <https://orcid.org/0009-0002-6405-2953>

Dwi Priyo Ariyanto  <https://orcid.org/0000-0001-6605-9599>

Sumani  <https://orcid.org/0000-0002-7488-2478>

References

- Alqudsi, Z. (2021). *Dinamika suhu udara dan suhu tanah pada berbagai tutupan lahan di KHDTK Gunung Bromo UNS Karanganyar*. [unpublished Bachelor thesis]. Universitas Sebelas Maret.
- Anshori, A., Srihartanto, E., Fibrianty, Suswatiningsih, T. E., Budiarti, S. W., Riyanto, D., Cahyaningrum, H., & Suradal. (2023). Increase of cropping index in dryland supported by groundwater irrigation. *Caraka Tani: Journal of Sustainable Agriculture*, 38(1), 1-13. <https://doi.org/10.20961/carakatani.v38i1.58029>
- Anusha, B. N., Babu, K. R., Kumar, B. P., Kumar, P. R., & Rajasekhar, M. (2022). Geospatial approaches for monitoring and mapping of water resources in semi-arid regions of Southern India. *Environmental Challenges*, 8, Article 100569. <https://doi.org/10.1016/j.envc.2022.100569>
- Ardiputro, R., Hadiyani, R. R. R., & Setiono, S. (2016). Prediksi kekeringan dengan metode standardized precipitation index (SPI) pada daerah aliran sungai Wuryantoro Kabupaten Wonogiri. [Drought prediction using the standardized precipitation index (SPI) method in the Wuryantoro River basin, Wonogiri Regency]. *Matriks Teknik Sipil*, 4(2), 482-491. <https://doi.org/10.20961/mateksi.v4i2.37003>
- Azadi, H., Keramati, P., Taheri, F., Rafiaani, P., Teklemariam, D., Gebrehiwot, K., Hosseininia, G., Passel, S. V., Lebailly, P., & Witlox, F. (2018). Agricultural land conversion: Reviewing drought impacts and coping strategies. *International Journal of Disaster Risk Reduction*, 31, 184-195. <https://doi.org/10.1016/j.ijdr.2018.05.003>
- Bhandari, A. K., Kumar, A., & Singh, G. K. (2012). Feature extraction using normalized difference vegetation index (NDVI): a case study of Jabalpur City. *Procedia Technology*, 6, 612-621. <https://doi.org/10.1016/j.protcy.2012.10.074>
- Bhavya, V. P., Kumar, S. A., Alur, A., Shivanna, M., & Shivakumar, K. M. (2018). Changes in soil physical properties as a result of different land use systems with depth. *International Journal of Current Microbiology and Applied Sciences*, 7(1), 323-327. <https://doi.org/10.20546/ijcmas.2018.701.035>
- Central Bureau of Statistics of Wonogiri Regency. (2022). *Kecamatan Manyaran dalam angka 2022*. <https://wonogirikab.bps.go.id/id/publication/2022/09/26/1656f6584f80ce75b405936c/kecamatan-manyaran-dalam-angka-2022.html>
- Chaniago, I., Syarif, A., & Riviona, P. (2017). Sorghum seedling drought response: In search of tolerant genotypes. *International Journal of Advance Science Engineering Information Technology*, 7(3), 892-897.
- Chaudhari, S. K., Bardhan, G., Kumar, P., Singh, R., Mishra, A. K., Rai, P., Singh, K. & Sharma, D. K. (2015). Short-term tillage and residue management impact on physical

- properties of a reclaimed sodic soil. *Journal of the Indian Society of Soil Science*, 63(1), 30-38. <https://doi.org/10.5958/0974-0228.2015.00005.5>
- Congalton, R. G. (1991). A review of assessing the accuracy of classifications of remotely sensed data. *Remote Sensing of Environment*, 37(1), 35-46. [https://doi.org/10.1016/0034-4257\(91\)90048-B](https://doi.org/10.1016/0034-4257(91)90048-B)
- Dariah, A., & Heryani, N. (2014). Pemberdayaan lahan kering suboptimal untuk mendukung kebijakan diversifikasi dan ketahanan pangan. [Sub-optimal dry land empowerment to support diversification and food security policies]. *Jurnal Sumberdaya Lahan*, 8(3), 1-16. <https://doi.org/10.2018/jsdl.v8i3.6477>
- Deng, Y., Wang, S., Bai, X., Tian, Y., Wu, L., Xiao, J., Chen, F. & Qian, Q. (2018). Relationship among land surface temperature and LUCC, NDVI in typical karst area. *Scientific Reports*, 8(1), Article 641. <http://10.1038/s41598-017-19088-x>
- Ding, N., Bai, Y., & Zhou, Y. (2023). Tree species mixtures can improve the water storage of the litter – soil continuum in subtropical coniferous plantations in China. *Forest*, 14(2), Article 431. <https://doi.org/10.3390/f14020431>
- Domiri, D. D. (2006). Pengembangan model pendugaan kelengasan tanah menggunakan data MODIS. [Development of soil moisture estimation model using MODIS data]. *Jurnal Penginderaan Jauh dan Pengolahan Data Citra Digital*, 3(1), 15-25.
- El-Nagar, D. A., & Mohamed, R. A. A. (2019). Characterization and impact of cattle manure particle size on physical properties of sandy soils. *Journal of Geoscience and Environment Protection*, 7(8), 180-194. <https://doi.org/10.4236/gep.2019.78013>
- Fujihara, Y., Yamada, R., Oda, M., Fujii, H., Ito, O., & Kashiwagi, J. (2013). Effects of puddling on percolation and paddy yields in rainfed lowland paddy cultivation: case study in Khammouane Province, Central Laos. *Agricultural Science*, 4(8), 360-368. <https://doi.org/10.4236/as.2013.48052>
- Gandhi, G. M., Parthiban, S., Thummalu, N., & Christy, A. (2015). NDVI: vegetation change detection using remote sensing and gis - a case study of Vellore District. *Procedia Computer Science*, 57, 1199-1210. <https://doi.org/10.1016/j.procs.2015.07.415>
- Goonetilleke, A., & Vithanage, M. (2017). Water resources management: innovation and challenges in a changing world. *Water*, 9(4), Article 281. <https://doi.org/10.3390/w9040281>
- Hakimi, F., & Hamdoun, F. Z. (2023). A multi-criteria sustainability assessment of mediterranean rainfed farming systems using the IDEA method: A Moroccan case study. *Caraka Tani: Journal of Sustainable Agriculture*, 38(2), 339-358. <https://doi.org/10.20961/carakatani.v38i2.75853>
- Hidayati, I. N. (2013). Ekstraksi data indeks vegetasi untuk evaluasi ruang terbuka hijau berdasarkan citra alos di Kecamatan Ngaglik Kabupaten Sleman Yogyakarta. [Extraction of vegetation index data for evaluation of green open spaces based on alos imagery in Ngaglik District, Sleman Regency, Yogyakarta]. *Jurnal Agroteknologi*, 3(2), 27-34. <http://doi.org/10.24014/ja.v3i2.85>
- Hugar, G. M., Sorganvi, V., & Hiremath, G. M. (2012). Effect of organic carbon on soil moisture. *Indian Journal of Natural Science*, 3(15), 1191-1235.
- Jones, H. G., & Vaughan, R. A. (2010). *Remote sensing of vegetation: Principles, techniques, and applications*. Oxford University Press.
- Karnieli, A., Agam, N., Pinker, R. T., Anderson, M., Imhoff, M. L., Gutman, G. G., Panov, N., & Alexander, G. (2010). Use of NDVI and land surface temperature for drought assessment: merits and limitations. *Journal of Climate*, 23(3), 618-633. <https://doi.org/10.1175/2009JCLI2900.1>
- Khanh, P. T., Ngoc, T. T. H., & Thuong, D. H. (2020). Application of landsat 8 image to extract waterline and built the relationship between chlorophyll-a and NDVI inde for

- Bung Binh Thien Lake, Southern Vietnam. *The International Journal of Engineering and Science*, 9(4), 20-28. <https://doi.org/10.9790/1813-0904032028>
- Kurniawan, I. D., Kinasih, I., Akbar, R. T. M., Chaidir, L., Iqbal, S., Pamungkas, B., & Imanudin, Z. (2023). Arthropod community structure indicating soil quality recovery in the organic agroecosystem of Mount Ciremai National Park's Buffer Zone. *Caraka Tani: Journal of Sustainable Agriculture*, 38(2), 229-243. <https://doi.org/10.20961/carakatani.v38i2.69384>
- Ladányi, Z., Barta, K., Blanka, V., & Pálffy, B. (2021). Assessing available water content of sandy soils to support drought monitoring and agricultural water management. *Water Resources Management*, 35, 869-880. <https://doi.org/10.1007/s11269-020-02747-6>
- Li, Y., Abdelkareem, M., & Al-Arifi, N. (2023). Mapping potential water resource areas using GIS-based frequency ratio and evidential belief function. *Water*, 15(3), Article 480. <https://doi.org/10.3390/w15030480>
- Libanda, B., Mie, Z., & Ngonga, C. (2019). Spatial and temporal patterns of drought in Zambia. *Journal of Arid Land*, 11, 180-191. <https://doi.org/10.1007/s40333-019-0053-2>
- Lin, G., Xia, B., Zeng, Z., & Huang, W. (2008). The relationship between NDVI, stand age, and terrain factors of *Pinus elliottii* forest. In *Proceedings of the 2008 international workshop on education technology and training & 2008 international workshop on geoscience and remote sensing* (Vol. 2, pp. 232-236). IEEE. <https://doi.org/10.1109/ETTandGRS.2008.302>
- Lund, J., Medellin-Azuara, J., Durand, J., & Stone, K. (2018). Lessons from California's 2012 – 2016 drought. *Journal of Water Resources Planning and Management*, 144(10), Article 04018067. [https://doi.org/10.1061/\(ASCE\)WR.1943-5452.0000984](https://doi.org/10.1061/(ASCE)WR.1943-5452.0000984)
- Mangani, T., Mangani, R., Chirima, G., Khomo, L., & Truter, W. (2022). Using mulching to reduce soil surface temperature to facilitate grass production. *Heliyon*, 8(12), Article e12284. <https://doi.org/10.1016/j.heliyon.2022.e12284>
- Meyer, N., Bergez, J.-E., Constantin, J. & Justes, E. (2019). Cover crops reduce water drainage in temperate climates: A meta-analysis. *Agronomy for Sustainable Development*, 39, Article 3. <https://doi.org/10.1007/s13593-018-0546-y>
- Minasny, B., & McBratney, A. B. (2017). Limited effect of organic matter on soil available water capacity. *European Journal of Soil Science*, 69(1), 39-47. <https://doi.org/10.1111/ejss.12475>
- Mohajane, M., Essahlaoui, A., Oudija, F., Hafyani, M. E., & Teodoro, A. C. (2017). Mapping forest species in the Central Middle Atlas of Morocco (Azrou Forest) through remote sensing techniques. *ISPRS International Journal of Geo-Information*, 6(9), Article 275. <https://doi.org/10.3390/ijgi6090275>
- Mohanty, M., Painuli, D. K., & Mandal, K. G. (2004). Effect of puddling intensity on temporal variation in soil physical conditions and yield of paddy (*Oryza sativa* L.) in a vertisol of Central India. *Soil and Tillage Research*, 76(2), 83-94. <https://doi.org/10.1016/j.still.2003.08.006>
- Monfared, S. A. H., Rezapour, M., & Zhian, T. (2019). Using windbreaks for decreasing lake and reservoir evaporation: a case study from Iran. *Polish Journal of Environmental Studies*, 28(4), 2289-2298. <https://doi.org/10.15244/pjoes/89984>
- Munir, M. M., Sasmito, B., & Haniah, H. (2015). Analisis pola kekeringan lahan pertanian di Kabupaten Kendal dengan menggunakan algoritma Thermal Vegetation Index dari citra satelit Modis Terra. [Analysis of agricultural land drought patterns in Kendal Regency using the Thermal Vegetation Index algorithm from Modis Terra satellite imagery]. *Jurnal Geodesi Undip*, 4(4), 174-180. <https://doi.org/10.14710/jgundip.2015.9943>
- Neamah, W. H., Sayed, S.F. A., & Hasan, F. A. (2023). Role of *Ocimum basilicum* var. *thrysiflora* (Thai Basil) aqueous extract treated with yeast suspension in enhancing tomato plant resistance to fusarium oxysporum. *Caraka Tani: Journal of Sustainable Agriculture*, 39(1), 38-47. <https://doi.org/10.20961/carakatani.v39i1.78387>

- Nuridin. (2011). The use of upland in Limboto watershed of Gorontalo Province for agriculture sustainability. *Jurnal Litbang Pertanian*, 30(3), 98-107.
- Orhan, O., Ekercin, S., & Dadaser-Celik, F. (2014). Use of Landsat land surface temperature and vegetation indices for monitoring drought in the Salt Lake Basin Area, Turkey. *The Scientific World Journal*, 2014, Article 142939. <https://doi.org/10.1155/2014/142939>
- Pandey, V., Srivastava, P. K., Singh, S. K., Petropoulos, G. P., & Mall, R. K. (2021). Drought identification and trend analysis using long-term chirps satellite precipitation product in Bundelkhand, India. *Sustainability*, 13(3), Article 1042. <https://doi.org/10.3390/su13031042>
- Qi, Z., Jingfang, S., & Wenwei, L. (2018). A survey about characteristics of soil water retention curve. In *2nd international workshop on renewable energy and development* (pp. 1-5). IOP Conference Series: Earth and Environmental Science, IOP Publishing. <https://doi.org/10.1088/1755-1315/153/6/062076>
- Rahayu, R., Supriyadi, S., Sumani, S., Herawati, A., Dewi, K. M., Mo, Y. G., & Bae, E. J. (2024). Assessment of land quality for siamese orange (*Citrus nobilis* var. *microcarpa*) development in Pacitan Regency, Indonesia. *AgriHealth: Journal of Agri-food, Nutrition and Public Health*, 5(1), 29-40. <https://doi.org/10.20961/agrihealth.v5i1.80729>
- Rahmawati, R. W. E., Hadiani, R. R. R., & Solichin, S. (2019). Analisis kekeringan hidrologi berdasarkan metode moisture adequacy index (MAI) di Daerah Aliran Sungai Temon Kabupaten Wonogiri. [Analysis of hydrological drought based on the moisture adequacy index (MAI) method in the Temon River Watershed, Wonogiri Regency]. *Matriks Teknik Sipil*, 7(3), 189-196. <https://doi.org/10.20961/mateksi.v7i3.36488>
- Rajeshwari, A., & Mani, N. D. (2014). Estimation of land surface temperature of Dindigul District using landsat 8 data. *International Journal of Research in Engineering and Technology*, 3(5), 122-126. <https://doi.org/10.15623/ijret.2014.0305025>
- Robinson, D. A., Jones, S. B., Lebron, I., Reinsch, S., Domínguez, M. T., Smith, A. R., Jones, D. L., Marshall, M. R., & Emmett, B. A. (2016). Experimental evidence for drought induced alternative stable states of soil moisture. *Scientific Report*, 6(2016), Article 20018. <https://doi.org/10.1038/srep20018>
- Romadhon, M. R., & Aziz, A. (2022). Determination of flood susceptibility index using overlay-scoring data method based on geographic information system (GIS) in Semarang city, Central Java, Indonesia. *AgriHealth: Journal of Agri-food, Nutrition and Public Health*, 3(2), 104-123. <https://doi.org/10.20961/agrihealth.v3i2.60451>
- Rusdin, I., Laga, A., Pirman, P., Sulaiman, M. R. R. A., & Irwan, I. (2023). Proximate characteristics of low glycemic index instant rice with variations in storage temperature and drying time. *AgriHealth: Journal of Agri-food, Nutrition and Public Health*, 4(2), 112-120. <https://doi.org/10.20961/agrihealth.v4i2.72099>
- Ryadi, G. Y. I., Sukmono, A., & Sasmito, B. (2019). Pengaruh fenomena el nino dan la nina pada persebaran curah hujan dan tingkat kekeringan lahan di Pulau Bali. [The influence of the El Nino and La Nina phenomena on the distribution of rainfall and the level of land drought on the island of Bali]. *Jurnal Geodesi Undip*, 8(4), 41-49. <https://doi.org/10.14710/jgundip.2019.25143>
- Sengupta, A., & Thangavel, M. (2023). Analysis of the effects of climate change on cotton production in Maharashtra State of India using statistical model and GIS mapping. *Caraka Tani: Journal of Sustainable Agriculture*, 38(1), 152-162. <https://doi.org/10.20961/carakatani.v38i1.64377>
- Silva, G. F. C., Gonçalves, A. C. A., da Silva, C. A. Jr., Nanni, M. R., Facco, C. U., Cezar, E. & da Silva, A. A. (2016). NDVI response to water stress in different phenological stages in culture bean. *Journal of Agronomy*, 15(1), 1-10. <https://doi.org/10.3923/ja.2016.1.10>

- Sruthi, S., & Aslam, M. A. M. (2015). Agricultural drought analysis using the NDVI and land surface temperature data; a case study of Raichur District. *Aquatic Procedia*, 4, 1258-1264. <https://doi.org/10.1016/j.aqpro.2015.02.164>
- Tatisina, N. N., Siahaya, W. A., & Haumahu, J. P. (2020). Transformasi Indeks Vegetasi Citra LANDSAT 8 OLI untuk pemetaan musim tanam pada lahan sawah di Kabupaten Buru, Provinsi Maluku. [Transformation of the LANDSAT 8 OLI Image Vegetation Index for mapping the planting season on rice fields in Buru Regency, Maluku Province]. *Jurnal Budidaya Pertanian*, 16(2), 197-205. <https://doi.org/10.30598/jbdp.2020.16.2.197>
- Taufik, M., & Setiawan, B. I. (2012). Interpretation of soil water content into dryness index : implication for forest fire management. *Jurnal Manajemen Hutan Tropika*, 18(1), 31-38. <https://doi.org/10.7226/jtfm.18.1.31>
- USGS. (2015). *Landsat 8 data users handbook*. <https://www.usgs.gov/landsat-missions/landsat-8-data-users-handbook>
- Utami, A. W., Widjanarko, N. P. A., Indradewa, D., Dhamira, A., Arum, M. R., Rizqi, F. A., Komarudin, N. A. & Prabaningtyas, D. (2024). Traditional ecological knowledge and farm household resilience to natural hazards. *Caraka Tani: Journal of Sustainable Agriculture*, 39(1), 154-166. <https://doi.org/10.20961/carakatani.v39i1.79774>
- van Genuchten, M. T. (1980). A closed-form equation for predicting the hydraulic conductivity of unsaturated soils. *Soil Science Society of America Journal*, 44(5), 892-898. <https://doi.org/10.2136/sssaj1980.03615995004400050002x>
- Veste, M., Littmann, T., Kunneke, A., Toit, B. D., & Seifert, T. (2020). Windbreaks as part of climate-smart landscapes reduce evapotranspiration in vineyards, Western Cape Province, South Africa. *Plant, Soil and Environment*, 66(3), 119-127. <https://doi.org/10.17221/616/2019-PSE>
- Wahyuti, I. S., Zulaika, I., Supriyadi, S., & Tonabut, W. (2023). Precise land evaluation implementation of the regional spatial plan in the Sleman Regency to maintain human health and food security. *AgriHealth: Journal of Agri-food, Nutrition and Public Health*, 4(2), 81-92. <https://doi.org/10.20961/agrihealth.v4i2.67850>
- Xiao, R., Weng, Q., Ouyang, Z., Li, W., Schienke, E. W., & Zhang, Z. (2008). Land surface temperature variation and major factors in Beijing, China. *Photogrammetric Engineering and Remote Sensing*, 74(4), 451-461. <https://doi.org/10.14358/PERS.74.4.451>
- Yates, S. R., van Genuchten, M. T., Warrick, A. W., & Leij, F. J. (1992). Analysis of measured, predicted, and estimated hydraulic conductivity using the RETC computer program. *Soil Science Society of America Journal*, 56(2), 347-354. <https://doi.org/10.2136/sssaj1992.03615995005600020003x>
- Yeneneh, N., Elias, E., & Feyisa, G. L. (2022). Detection of land use/land cover and land surface temperature change in the Suha Watershed, North-Western highlands of Ethiopia. *Environmental Challenges*, 7, Article 100253. <https://doi.org/10.1016/j.envc.2022.100523>
- Yu, W., Wardrop, N. A., Bain, R. E. S., Alegana, V., Graham, L. J., & Wright, J. A. (2019). Mapping access to domestic water supplies from incomplete data in developing countries: An illustrative assessment for Kenya. *PLoS ONE*, 14(5), Article e0216923. <https://doi.org/10.1371/journal.pone.0216923>
- Zheng, K., Cheng, J., Xia, J., Liu, G., & Xu, L. (2021). Effects of soil bulk density and moisture content on the physico-mechanical properties of paddy soil in plough layer. *Water*, 13(16), Article 2290. <https://doi.org/10.3390/w13162290>